Nonlinear photonic crystal fibres: pushing the zero-dispersion toward the visible

Kunimasa Saitoh and Masanori Koshiba
Hokkaido University, North 14 West 9, Kita-ku, Sapporo, 060-0814, Japan

Niels Asger Mortensen§
MIC – Department of Micro and Nanotechnology, NanoDTU, Technical University of Denmark, Bld. 345 east, DK-2800 Kongens Lyngby, Denmark

Abstract. The strong waveguide dispersion in photonic crystal fibres provides unique opportunities for nonlinear optics with a zero-dispersion wavelength λ_0 far below the limit of $\sim 1.3\,\mu$m set by the material dispersion of silica. By tuning the air-hole diameter d, the pitch Λ, and the number of rings of air holes N, the strong waveguide dispersion can in principle be used to extend λ_0 well into the visible, albeit to some extend at the cost of multimode operation. We study in detail the interplay of the zero-dispersion wavelength, the cut-off wavelength λ_c, and the leakage loss in the parameter space spanned by d, Λ, and N. As a particular result we identify values of d ($\sim$ 500 nm) and Λ ($\sim$ 700 nm) which facilitate the shortest possible zero-dispersion wavelength ($\sim$ 700 nm) while the fibre is still single-mode for longer wavelengths.

PACS numbers: 42.70.Qs, 42.81.Dp, 42.81.-i

Submitted to: *New J. Phys. (Focus on Nanophotonics)*

§ Corresponding author: nam@mic.dtu.dk

1. Introduction

Photonic crystal fibres (PCFs) [1, 2] have led to an enormous renewed interest in nonlinear fibre optics [3, 4, 5]. In particular, the strong anomalous group-velocity dispersion has facilitated visible super-continuum generation [6], which apart from being a fascinating and rich non-linear phenomenon [7] also has promising applications including frequency-comb metrology [8, 9] and optical coherence tomography [10].

The regular triangular arrangement of sub-micron air-holes running along the full length of the fibre [11, 12], see Fig. 1, is a key concept for the realization of strong anomalous chromatic dispersion which arises in a competition between material dispersion and wave-guide dispersion originating from the strong transverse confinement of light. At the same time the strong transverse confinement of light also serves to dramatically decrease the effective area and increase the non-linear coefficient [13] so that very high optical intensities may be achieved relative to the input power.

The zero-dispersion wavelength may be tuned down to the visible [14, 15] by carefully increasing the normalized air-hole diameter d/Λ while at the same time decreasing the pitch Λ. However, in many cases the very short zero-dispersion wavelength is achieved at the cost of multi-mode operation. Furthermore, the reduction of the pitch may require a large number N of rings of air holes in order to circumvent leakage loss.

In this paper we in detail study the complicated interplay of the zero-dispersion wavelength λ_0, the cut-off wavelength λ_c, and the leakage loss in the parameter space spanned by d, Λ, and N. As a particular result we identify values of d and Λ which facilitate the shortest possible zero-dispersion wavelength while the fibre is still single-mode for longer wavelengths, i.e. $\lambda_c \leq \lambda_0$.

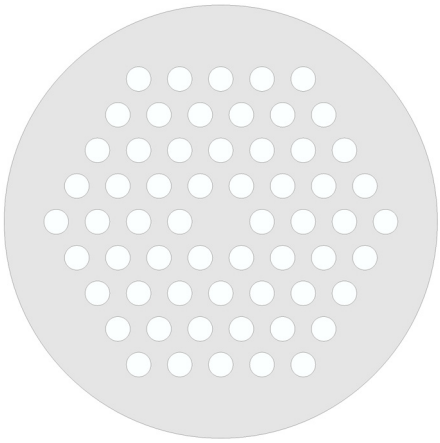

Figure 1. Cross section of a photonic crystal fibre with $N = 4$ rings of air holes in the photonic crystal cladding surrounding the core defect which is formed by the omission of a single air hole in the otherwise periodic structure. The photonic crystal cladding comprises air holes of diameter d arranged in a triangular array of pitch Λ.

2. Competition between material and wave-guide dispersion

The linear dynamics and response of a waveguide is typically studied within the framework of temporal harmonic modes, $\vec{E}(\vec{r},t) = \vec{E}(\vec{r}_\perp)e^{-i\omega t} = \vec{\mathcal{E}}(\vec{r}_\perp)e^{i(\beta z-\omega t)}$, where $\vec{E}(\vec{r})$ is a solution to the vectorial wave equation

$$\nabla \times \nabla \times \vec{E}(\vec{r}) = \varepsilon(\vec{r},\omega)\frac{\omega^2}{c^2}\vec{E}(\vec{r}). \tag{1}$$

Here, $\varepsilon(\vec{r},\omega) = n^2(\vec{r},\omega)$ is the spatially dependent dielectric function of the composite air-silica dielectric medium, see Fig. 1, and $n(\vec{r},\omega)$ is the corresponding refractive index.

Solving the wave equation, Eq. (1), provides us with the dispersion relation $\omega(\beta)$ which contains all information on the spatial-temporal linear dynamics of wave packets and it is furthermore important input for studies of non-linear dynamics. However, quite often the dynamics and evolution of pulses are quantified by the derived dispersion parameters $\beta_n = (\partial^n\omega/\partial^n\beta)^{-1}$ with $\beta_1 = v_g^{-1}$ being recognized as the inverse group velocity. The group-velocity dispersion β_2 is in fiber optics commonly quantified by the dispersion parameter D (typically in units of ps/nm/km) which can be written in a variety of ways including

$$D = \frac{\partial^2\beta}{\partial\lambda\partial\omega} = \frac{\partial\beta_1}{\partial\lambda} = -\frac{\omega^2}{2\pi c}\beta_2 \tag{2}$$

where $\lambda = 2\pi c/\omega$ is the free-space wavelength. The dispersion in the group velocity makes different components in a pulse propagate at different speeds and thus pulses

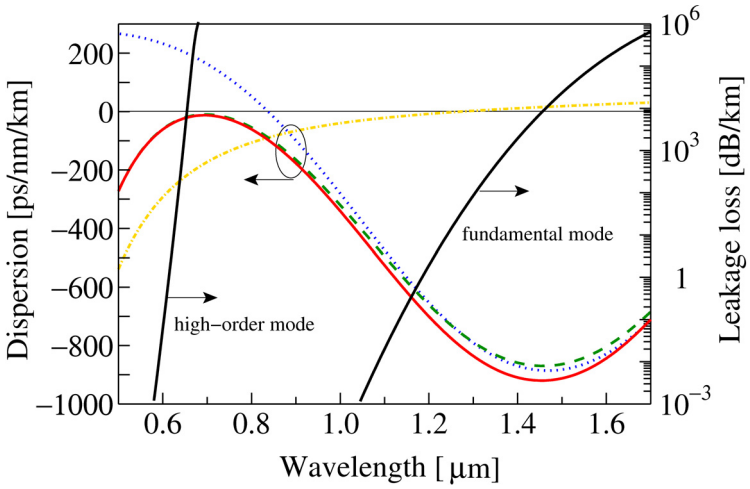

Figure 2. Left axis: Dispersion parameter versus wavelength for a photonic crystal fibre with $d/\Lambda = 0.7$, $\Lambda = 700\,\mathrm{nm}$, and $N = 10$. The solid curve shows the total dispersion, Eq. (2), obtained through a self-consistent numerical solution of the wave equation, Eq. (1), while the dashed line shows the approximate addition of waveguide and material dispersion, Eq. (7). The dotted curve shows the pure waveguide contribution, Eq. (5), while the dot-dashed curve shows the silica material dispersion, Eq. (6). Right axis: Leakage loss versus wavelength for the fundamental and the first high-order mode. The rapid increase in the leakage loss of the high-order mode marks the cut-off wavelength.

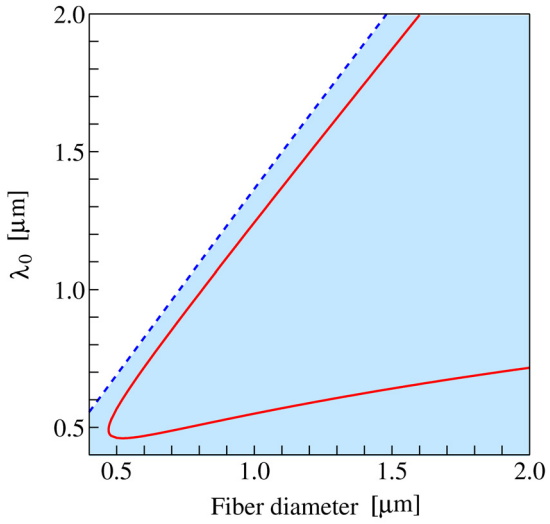

Figure 3. Zero-dispersion wavelength versus fibre diameter for a strand of silica in air. The dashed line indicates the cut-off wavelength and the blue shading indicates the multi-mode phase.

will compress or broaden in time depending on the sign of D. The zero-dispersion wavelength λ_0, defined by $D(\lambda_0) = 0$, is thus of particular relevance to pulse dynamics in general and non-linear super-continuum generation in particular. By pumping the fiber with high-intensive ultra-short nano and femto-second pulses near λ_0 the pump pulses will loosely speaking maintain their high intensity for a longer time (or propagation distance) thus allowing for pronounced non-linear interactions.

The finite group-velocity dispersion is a consequence of both the dispersive properties of the host material itself as well as the strong transverse localization of the light caused by the pronounced spatial variations in the dielectric function. Since the variation with frequency of the refractive index of silica is modest (at least in the transparent part of the spectrum) the dielectric function satisfies

$$\varepsilon(\vec{r}_\perp,\omega) \;= \varepsilon_0(\vec{r}_\perp,\tilde{\omega}) + \delta\varepsilon(\vec{r}_\perp,\omega), \tag{3}$$

$$\delta\varepsilon(\vec{r}_\perp,\omega) = \varepsilon(\vec{r}_\perp,\omega) - \varepsilon_0(\vec{r}_\perp,\tilde{\omega}) \ll \varepsilon_0(\vec{r}_\perp,\omega) \tag{4}$$

where $\tilde{\omega}$ is some arbitrary, but fixed frequency where consequently $\delta\varepsilon = 0$. The high attention to the telecommunication band has often made $\tilde{\lambda} = 1550\,\mathrm{nm}$ a typical choice, though this is by no means a unique choice. From ε_0 one may define a pure waveguide contribution D_w to the dispersion parameter by the definition

$$D_w = \frac{\partial^2 \beta_0}{\partial\lambda\partial\omega} \tag{5}$$

where $\beta_0(\omega)$ is the solution to the wave equation with $\varepsilon(\vec{r}_\perp,\omega) = \varepsilon_0(\vec{r}_\perp,\tilde{\omega})$, i.e. the frequency dependence of the dielectric function is ignored. Furthermore, this has the consequence that the wave equation, Eq. (1), becomes scale invariant which is very convenient from a numerical point of view since results for one characteristic length scale can easily be scaled to a different length scale.

For the dielectric material itself one likewise defines a material dispersion D_m by solving the wave equation with $\varepsilon(\vec{r}_\perp,\omega) = \varepsilon_m(\omega) = n_m^2(\omega)$. From the simple homogeneous-space dispersion relation it readily follows that

$$D_m = -\frac{\lambda}{c}\frac{\partial^2 n_m}{\partial \lambda^2}. \tag{6}$$

Intuitively, one might speculate that the two kinds of sources of dispersion simply add up and actually the approximation

$$D \approx D_w + D_m \tag{7}$$

is used widely in the literature. While the approximation is useful in qualitatively understanding the zero-dispersion properties it is however also clear (see e.g. the work of Ferrando *et al.* [16]) that quantitative correct results requires either a self-consistent solution of the wave equation or some accurate perturbative method [17, 18].

In this paper we use a fully self-consistent solution of the wave equation, Eq. (1). For the dielectric function we use the frequency-independent value $\varepsilon = 1$ in the air-hole regions while we for silica employ the usual three-term Sellmeier polynomial description,

$$\varepsilon_m(\lambda) = n_m^2(\lambda) = 1 + \sum_{j=1}^{3} \frac{a_j \lambda^2}{\lambda^2 - \lambda_j^2} \tag{8}$$

where the absorption lines λ_j and the corresponding strengths a_j are given by

$$\lambda_1 = 0.0684043\,\mu\text{m}, \qquad a_1 = 0.6961663, \tag{9}$$

$$\lambda_2 = 0.1162414\,\mu\text{m}, \qquad a_2 = 0.4079426, \tag{10}$$

$$\lambda_3 = 9.896161\,\mu\text{m}, \qquad a_3 = 0.8974794. \tag{11}$$

Figure 2 illustrates the typical dispersion properties of a photonic crystal fibre. The strongly negative material dispersion D_m of silica below $\lambda \sim 1.3\,\mu$m tend to make the total dispersion D of standard fibres negative for $\lambda \lesssim 1.3\,\mu$m, simply because of the very weak waveguide contribution D_w. However, photonic crystal fibres are contrary to this since the composite air-silica cladding is seen to provide the guided mode with a strongly positive waveguide dispersion D_w which tends to shift the zero-dispersion wavelength λ_0 far below $1.3\,\mu$m towards the visible. While the material dispersion is fixed the waveguide dispersion varies strongly in the phase-space spanned by d and Λ and in this way the competition between waveguide and material dispersion becomes a powerful mechanism in engineering the zero-dispersion wavelength.

3. A strand of silica in air — the ultimate limit?

As mentioned in the introduction the zero-dispersion wavelength may be pushed to lower values by simply increasing the air hole diameter and decreasing the pitch. For $d/\Lambda \to 1$ this will to some extend effectively leave us with a single strand of silica surrounded by air. This limiting case has been emphasized previously in the literature and in Fig. 3 we reproduce the zero-dispersion wavelength results reported by Knight *et al.* [14]. Generally, the strand of silica will have either two dispersion zeros or none, with the exception of the special case where it only supports a single dispersion zero. PCFs turn out to follow the same overall pattern and the existence of two dispersion zeros turns out to have interesting applications in super-continuum generation [19].

The results in Fig. 3 leave promises for a zero-dispersion wavelength down to below 500 nm which will eventually also be the ultimate limit for silica based PCFs. However, as also indicated by the dashed line the large index contrast between air and silica in general prevents single-mode operation at the zero-dispersion wavelength. In the following we will study to which degree the photonic crystal cladding concept of PCFs can be used to circumvent this problem.

4. Photonic crystal cladding as a modal sieve

As demonstrated already by Birks *et al.* [12] the photonic crystal cladding of a PCF acts as modal sieve which may prevent localization of high-order modes to the core region. This so-called endlessly single-mode property has later been studied in great detail [13, 20, 21, 22] and it was recently argued that the endlessly single-mode phenomena is a pure geometrical effect and that the PCF is endlessly single mode for $d/\Lambda \lesssim 0.42$ irrespectively of the fibre material refractive index [23]. The photonic crystal cladding thus serves to limit the number of guided modes and at the same time the guided modes will to some extend inherit the chromatic dispersion properties observed for the strand of silica in air [14].

The problem of zero-dispersion wavelength versus pitch has previously been studied for PCFs with an infinite photonic crystal cladding [18] demonstrating curves qualitatively resembling the curve in Fig. 3. Here, we extend that work to PCFs with a photonic crystal cladding of finite spatial extent. In particular, we study the effect of a varying number N of rings of air holes surrounding the core region. We also study the cut-off and leakage properties to explore the possibility for a single-mode PCF with a zero-dispersion wavelength in the visible.

Our numerical solutions of the wave equation, Eq. (1), are based on a finite-element approach which is described in detail in Ref. [24]. For the calculation of the cut-off wavelength and the leakage loss we refer to Refs. [25, 26] and references therein.

The results of extensive numerical simulations are summarized in Fig. 4. First of all we notice that the zero-dispersion wavelength versus pitch has a curve-shape qualitatively resembling the result in Fig. 3 for a strand of silica in air. Furthermore, we see that the number N of rings of air holes has little influence on the zero-dispersion wavelength. In particular, the results for $N = 10$ are in full quantitative agreement with those reported in Ref. [18]. On the other hand, the spatial extent $N \times \Lambda$ of the photonic crystal cladding is as expected seen to have a huge impact on the leakage loss [27, 26] as seen from the red shading indicating the region with a leakage loss exceeding 0.1 dB/km. Furthermore, N has as expected little effect on the cut-off wavelength since the cut-off and the modal sieving is governed by the width $(\Lambda - d)$ of the silica regions between the air holes [23] rather than the spatial extent $N \times \Lambda$ of the photonic crystal cladding.

Finally, we note that by choosing $d/\Lambda \sim 0.7$ we may realize a PCF with a single zero-dispersion wavelength down to $\sim$ 700 nm with the fibre being single-mode for longer wavelengths. We believe this to be the ultimate limit for silica-based PCFs having a photonic crystal cladding comprising a triangular arrangement of circular air holes. Such results have been demonstrated experimentally by e.g. Knight *et al.* [14]. In practice, the limit might be pushed slightly further toward the visible since real PCFs tend to have a slightly shorter cut-off wavelength compared to the expectations based on the ideal fibre structure [22]. Most likely, this tendency originates in the presence of scattering loss in real fibres which also acts in suppressing the high-

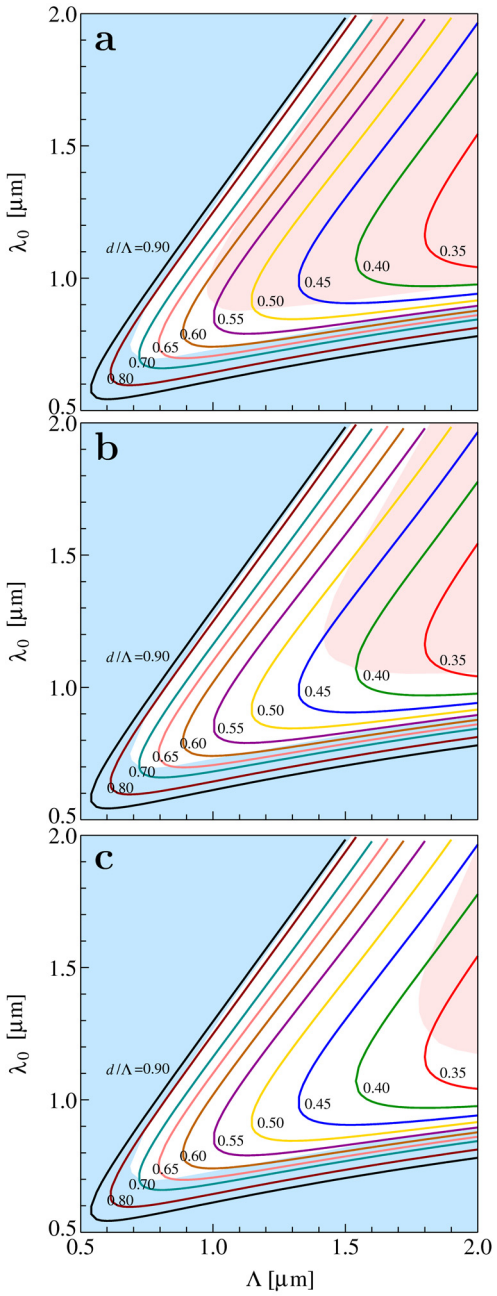

Figure 4. Zero-dispersion wavelength λ_0 versus pitch Λ for different values of the normalized air-hole diameter d/Λ. Panels a), b), and c) are for $N = 6, 8$, and 10 rings of air holes, respectively. Regions with a leakage loss larger than 0.1 dB/km are indicated by red shading. Similarly, the multi-mode regime is indicated by blue shading.

order modes even though they are weakly guided by the photonic crystal cladding. In order to push the zero-dispersion wavelength further into the visible one would have to tolerate guidance of high-order modes or alternatively employ somewhat more complicated designs involving a varying air-hole diameter throughout the cladding [28].

5. Conclusion

In conclusion we have studied the zero-dispersion wavelength λ_0 in silica based photonic crystal fibres with special emphasis on the interplay with the cut-off wavelength and leakage loss. In the large parameter space spanned by the air-hole diameter d and the pitch Λ we have identified the values facilitating the shortest possible zero-dispersion wavelength (~ 700 nm) while the fibre is still single-mode for longer wavelengths.

We believe that our λ_0-maps are an important input for the efforts in designing nonlinear photonic crystal fibres with still shorter zero-dispersion wavelengths for super-continuum generation in the visible.

6. Acknowledgments

N. A . M. acknowledges discussions with J. Lægsgaard as well as the collaboration on the zero-dispersion results in Ref. [18] which strongly stimulated the present work.

[1] Russell P S J 2003 *Science* **299** 358 – 362
[2] Knight J C 2003 *Nature* **424** 847 – 851
[3] Mollenauer L F 2003 *Science* **302** 996 – 997
[4] Hansen K P 2005 *Journal of Optical and Fiber Communications Reports* **2** 226 – 254 [doi: 10.1007/s10297-004-0021-1]
[5] Zheltikov A 2006 *J. Opt. A: Pure Appl. Opt.* **8** S47 – S72
[6] Ranka J K, Windeler R S and Stentz A J 2000 *Opt. Lett.* **25** 25 – 27
[7] Herrmann J, Griebner U, Zhavoronkov N, Husakou A, Nickel D, Knight J C, Wadsworth W J, Russell P S J and Korn G 2002 *Phys. Rev. Lett.* **88** 173901
[8] Jones D J, Diddams S A, Ranka J K, Stentz A, Windeler R S, Hall J L and Cundiff S T 2000 *Science* **288** 635 – 639
[9] Udem T, Holzwarth R and Hänsch T W 2002 *Nature* **416** 233 – 237
[10] Hartl I, Li X D, Chudoba C, Ghanta R K, Ko T H, Fujimoto J G, Ranka J K and Windeler R S 2001 *Opt. Lett.* **26** 608 – 610
[11] Knight J C, Birks T A, Russell P S J and Atkin D M 1996 *Opt. Lett.* **21** 1547 – 1549
[12] Birks T A, Knight J C and Russell P S J 1997 *Opt. Lett.* **22** 961 – 963
[13] Mortensen N A 2002 *Opt. Express* **10** 341 – 348
[14] Knight J C, Arriaga J, Birks T A, Ortigosa-Blanch A, Wadsworth W J and Russell P S J 2000 *IEEE Phot. Technol. Lett.* **12** 807 – 809
[15] Skryabin D V, Luan F, Knight J C and Russell P S J 2003 *Science* **301** 1705 – 1708
[16] Ferrando A, Silvestre E, Miret J J and Andres P 2000 *Opt. Lett.* **25** 790 – 792
[17] Lægsgaard J, Bjarklev A and Libori S E B 2003 *J. Opt. Soc. Am. B* **20** 443 – 448
[18] Lægsgaard J, Mortensen N A and Bjarklev A 2003 *J. Opt. Soc. Am. B* **20** 2037 – 2045
[19] Andersen T V, Hilligsøe K M, Nielsen C K, Thøgersen J, Hansen K P, Keiding S R and Larsen J J 2004 *Opt. Express* **12** 4113 – 4122
[20] Kuhlmey B T, McPhedran R C and de Sterke C M 2002 *Opt. Lett.* **27** 1684 – 1686
[21] Mortensen N A, Folkenberg J R, Nielsen M D and Hansen K P 2003 *Opt. Lett.* **28** 1879 – 1881
[22] Folkenberg J R, Mortensen N A, Hansen K P, Hansen T P, Simonsen H R and Jakobsen C 2003 *Opt. Lett.* **28** 1882 – 1884
[23] Mortensen N A 2005 *Opt. Lett.* **30** 1455 – 1457
[24] Koshiba M 2002 *IEICE Trans. Electron.* **85-C** 881 – 888
[25] Saitoh K, Tsuchida Y, Koshiba M and Mortensen N A 2005 *Opt. Express* **13** 10833 – 10839
[26] Koshiba M and Saitoh K 2005 *Opt. Commun.* **253** 95 – 98
[27] White T P, McPhedran R C, de Sterke C M, Botten L C and Steel M J 2001 *Opt. Lett.* **26** 1660 – 1662
[28] Jacobsen R S, Lægsgaard J, Bjarklev A and Hougaard K 2004 *J. Opt. A: Pure Appl. Opt.* **6** 604 – 607